January 1998

Detection of Center Vortices in the Lattice Yang-Mills Vacuum

L. Del Debbio[a], *M. Faber*[b], *J. Giedt*[c], *J. Greensite*[d], *and Š. Olejník*[e]

[a] Dept. of Physics and Astronomy, Univ. of Southampton, Southampton SO17 1BJ, UK. E-mail: ldd@hep1.phys.soton.ac.uk

[b] Inst. für Kernphysik, Technische Universität Wien, A-1040 Vienna, Austria. E-mail: faber@kph.tuwien.ac.at

[c] Physics Department, University of California, Berkeley, CA 94720 USA. E-mail: giedt@socrates.berkeley.edu

[d] The Niels Bohr Institute, DK-2100 Copenhagen Ø, Denmark. E-mail: greensite@nbivms.nbi.dk

[e] Institute of Physics, Slovak Academy of Sciences, SK-842 28 Bratislava, Slovakia. E-mail: fyziolej@savba.sk

Abstract

We discuss the implementation of the "direct" maximal center gauge (a gauge which maximizes the lattice average of the squared-modulus of the trace of link variables), and its use in identifying Z_2 center vortices in Yang-Mills vacuum configurations generated by lattice Monte Carlo. We find that center vortices identified in the vacuum state account for the full asymptotic string tension. Scaling of vortex densities with lattice coupling, change in vortex size with cooling, and sensitivity to Gribov copies is discussed. Preliminary evidence is presented, on small lattices, for center dominance in $SU(3)$ lattice gauge theory.

1 Introduction

In a number of recent articles and conference proceedings [1–3] we have presented numerical evidence in favor of the Center Vortex theory of confinement, which was put forward in the late 1970's [4–8]. Our most important tool is the use of the maximal center gauge, which, combined with "center projection," allows us to identify the locations of center vortices in thermalized lattice gauge-field configurations. It is found that these vortices, by themselves, account for the entire asymptotic string tension ("center dominance"). We have also found evidence [2] that the monopoles of the maximum abelian gauge lie along the center vortices in a monopole-antimonopole chain, and that their non-abelian field strength, above the vacuum average, is almost entirely oriented in the vortex direction. This opens the way to explain abelian dominance, and monopole condensation, in terms of more fundamental underlying vortex configurations. Finally, in ref. [9], we have argued that the Casimir scaling of higher representation string tensions, formerly a very strong argument *against* the center vortex theory, can in fact be understood in terms of center vortices. Independent arguments in favor of the center vortex theory have been presented by Kovács and Tomboulis [10], who follow a rather different approach but reach similar conclusions.

In this article we will explain, in section 2, the actual implementation of the "direct" maximal center gauge, which underlies much of our work, and review the evidence, in the direct gauge, that center vortices are responsible for quark confinement.[1] We go on to study (section 3) how vortex configurations are affected by cooling the lattice, and then take up issues related to Gribov copies (section 4). Some preliminary evidence for center dominance in $SU(3)$ lattice gauge theory is presented in section 5, followed by a summary of our results in section 6.

2 Center Vortices and Confinement

Our procedure for locating center vortices in thermalized lattice configurations was inspired by earlier work on abelian projection in maximal abelian gauge [11]. The idea is to fix a gauge (the maximal center gauge) which, in the case of $SU(2)$ gauge theory, reduces the full $SU(2)$ gauge symmetry to the center subgroup Z_2. "Center projection" is a mapping of the full gauge field configuration $U_\mu(x)$ onto a configuration $Z_\mu(x) = \pm 1$, transforming as a Z_2 gauge field under the residual Z_2 symmetry. The excitations of a Z_2 gauge field are (thin) center vortices, and these are used to locate thick center vortices in the full, unprojected gauge-field configuration $U_\mu(x)$, as explained below.

In fact we have introduced two versions of the maximal center gauge; an "indirect" version, in refs. [1, 12], and a "direct" maximal center gauge in ref. [2]. The indirect gauge is a further gauge-fixing within maximal abelian gauge, which reduces the residual $U(1)$ gauge symmetry to Z_2. One begins by fixing to maximal abelian gauge, defined as the

[1] Some of this evidence was obtained previously in a slightly different, "indirect", version of maximal center gauge [1, 2].

gauge which maximizes

$$Q = \sum_{x,\mu} \mathrm{Tr}[U_\mu(x)\sigma_3 U_\mu^\dagger(x)\sigma_3] \tag{1}$$

leaving a residual $U(1)$ symmetry. This gauge makes the link variables as diagonal as possible. Abelian link variables are extracted from the diagonal elements of the full link variables, rescaled to restore unitarity:

$$\begin{aligned} A &= \frac{\mathrm{diag}[U_{11}, U_{22}]}{\sqrt{U_{11}U_{11}^* + U_{22}U_{22}^*}} \\ &= \begin{bmatrix} e^{i\theta} & \\ & e^{-i\theta} \end{bmatrix} \end{aligned} \tag{2}$$

These variables transform under the residual symmetry like $U(1)$ gauge field link variables. The indirect maximal center gauge uses this residual symmetry to bring the A-link variables as close as possible to $SU(2)$ center elements $\pm I$, by maximizing the lattice average of $\cos^2(\theta)$. Center projection is then achieved by identifying

$$Z_\mu(x) = \mathrm{sign}[\cos(\theta_\mu(x))] \tag{3}$$

The gauge is "indirect" in the sense that the center is maximized in the abelian link variable A, rather than directly in the full link variable U. String tensions can be extracted from the center-projected configurations and, although agreement with the asymptotic string tension of the full configurations is not too bad, significantly better results are obtained in the direct maximal center gauge, as will be seen below.

The direct maximal center gauge, in $SU(2)$ gauge theory, is defined as the gauge which brings the full link variables U as close as possible to the center elements $\pm I$, by maximizing the quantity

$$R = \sum_{x,\mu} \mathrm{Tr}[U_\mu(x)]^2 \tag{4}$$

with center projection defined by

$$Z_\mu(x) = \mathrm{sign}[\mathrm{Tr}U_\mu(x)] \tag{5}$$

Again, the projected $Z_\mu(x)$ field transforms as a gauge field under the residual Z_2 symmetry. Before going on to discuss numerical results obtained in this gauge, we must first discuss how to implement it.

2.1 Fixing to direct maximal center gauge

The gauge-fixing is accomplished by over-relaxation [13]. Beginning with a thermalized but non-gauge-fixed lattice, we sweep through the lattice site by site. At each site x, one needs to find the gauge transformation g which maximizes the local quantity

$$R_x = \frac{1}{4}\left\{ \sum_\mu \mathrm{Tr}[g(x)U_\mu(x)]^2 + \sum_\mu \mathrm{Tr}[U_\mu(x-\hat{\mu})g^\dagger(x)]^2 \right\} \tag{6}$$

Denote

$$\begin{aligned} g(x) &= g_4 I - i\vec{g}\cdot\vec{\sigma} \\ U_\mu(x) &= d_4(\mu) I + i\vec{d}(\mu)\cdot\vec{\sigma} \\ U_\mu(x-\hat{\mu}) &= d_4(\mu+4) I - i\vec{d}(\mu+4)\cdot\vec{\sigma} \end{aligned} \tag{7}$$

where the choice of signs in front of the various terms proportional to i is made for convenience. Then

$$R_x = \frac{1}{2}\sum_{l=1}^{8}\left(\sum_{k=1}^{4} g_k d_k(l)\right)^2 \tag{8}$$

We have to maximize this quantity subject to the constraint that g is unitary. To this end, introduce a Lagrange multiplier

$$\tilde{R} = R_x + \frac{1}{2}\lambda\left(1 - \sum_{k=1}^{4} g_k^2\right) \tag{9}$$

Then the conditions for a maximum satisfying the constraint, obtained by differentiating $\tilde{R}$, are

$$\begin{aligned} \sum_{j=1}^{4}\sum_{l=1}^{8} d_i(l) d_j(l) g_j &= \lambda g_i \\ \sum_{k=1}^{4} g_k^2 &= 1 \end{aligned} \tag{10}$$

This can be written as an eigenvalue equation

$$D\vec{G} = \lambda\vec{G} \tag{11}$$

where

$$D_{ij} = \sum_{l=1}^{8} d_i(l) d_j(l) \tag{12}$$

and the unitarity constraint is the normalization condition

$$\vec{G}\cdot\vec{G} = 1 \tag{13}$$

At this point, the problem of finding g boils down to finding the eigenvectors of a 4×4 real symmetric matrix, which is achieved by standard methods. There are four eigenvectors corresponding to four stationary points. The eigenvector with the largest eigenvalue corresponds to the gauge transformation g maximizing R_x at site x.

The next step is to apply the over-relaxation algorithm. We transform the links touching site x not by $g(x)$ but by $g^\omega(x)$, where

$$\begin{aligned} g &= g_4 I - i\vec{g}\cdot\vec{\sigma} \\ &= \cos(\phi) I - i\vec{n}\cdot\vec{\sigma}\sin(\phi) \\ g^\omega &= \cos(\omega\phi) I - i\vec{n}\cdot\vec{\sigma}\sin(\omega\phi) \end{aligned} \tag{14}$$

and we use $\omega = 1.7$ [13]. This procedure is applied at each site of the lattice, sweeping through the lattice several hundred times. The algorithm stops when a convergence criterion is satisfied. Our criterion is that the lattice average of $(\frac{1}{2}\mathrm{Tr}U)^2$ changes by less than 0.00015 after 50 gauge-fixing sweeps.

Finally, it must be noted that maximal center gauge, like the Coulomb, Landau, and maximal abelian gauges, is afflicted with Gribov copies. To alleviate the problem, we make several gauge copies of the original configuration by applying random gauge transformations, and then gauge fix each copy. The gauge-fixed copy with the largest value of R is chosen for data-taking. In practice, three gauge copies seems sufficient, in the sense that we don't improve the average value of R very much (or change the final results) by making more copies.

All of the data reported below was obtained in the direct maximal center gauge. A portion of those results, displayed in Figures 1-7 below, are similar to results obtained previously in the indirect version of maximal center gauge [1].

2.2 Projection vortices locate center vortices

Having fixed to the direct maximal center gauge by this procedure, we obtain the corresponding center-projected configuration (a Z_2 lattice gauge field), from (5). The excitations of any Z_2 gauge field are line-like (D=3) or surface-like (D=4) vortices on the dual lattice. We refer to these excitations, in the center-projected configurations, as "projection vortices" or just "P-vortices." The question is whether P-vortices in the projected configuration are in any way related to the existence of center vortices in the full, unprojected lattice configuration.

In order to study this question, we introduce the concept of vortex-limited Wilson loops $W_n(x)$. We say that a plaquette is pierced by a P-vortex if, upon going to maximal center gauge and center-projecting, the projected plaquette has the value -1. Likewise, a given lattice surface is pierced by n P-vortices if n plaquettes of the surface are pierced by P-vortices. As a Monte Carlo simulation proceeds, the number of P-vortices piercing any given surface will vary. Define $W_n(C)$ to be the Wilson loop evaluated on a sub-ensemble of configurations, selected such that precisely n P-vortices, in the corresponding center-projected configurations, pierce the minimal area of the loop. It should be emphasized here that the center projection is used only to select the data set. The Wilson loops themselves are evaluated using the full, *unprojected* link variables. In practice, to compute $W_n(C)$, the procedure is to generate thermalized lattice configurations by the usual Monte Carlo algorithm, and fix to maximal center gauge as described above. For each independent configuration one then examines each rectangular loop on the lattice of a given size; those with n P-vortices piercing the loop are evaluated, the others are skipped.

The test for whether (thin) P-vortices in the projected configuration correspond to (thick) center vortices in the full, unprojected $SU(2)$ gauge-field configuration is whether the behavior

$$\frac{W_n(C)}{W_0(C)} \to (-1)^n \tag{15}$$

is found in the limit of large loop area. The reasoning behind this test has been given elsewhere [1, 2], but for completeness we repeat the argument here.

Vortices are created by discontinuous gauge transformations. Suppose loop C, parametrized by $x^\mu(\tau),\ \tau \in [0,1]$, encircles n vortices. At the point of discontinuity

$$g(x(0)) = (-1)^n g(x(1)) \tag{16}$$

The corresponding vector potential, in the neighborhood of loop C can be decomposed as

$$A_\mu^{(n)}(x) = g^{-1}\delta A_\mu^{(n)}(x) g + i g^{-1}\partial_\mu g \tag{17}$$

with the inhomogenous term dropped at the point of discontinuity. Then

$$\begin{aligned} W_n(C) &= < \mathrm{Tr} \exp[i \oint dx^\mu A_\mu^{(n)}] > \\ &= (-1)^n < \mathrm{Tr} \exp[i \oint dx^\mu \delta A_\mu^{(n)}] > \end{aligned} \tag{18}$$

In the region of the loop C, the vortex background looks locally like a gauge transformation. If all other fluctuations $\delta A_\mu^{(n)}$ are basically short-range, then they should be oblivious, in the neighborhood of the loop C, to the presence or absence of vortices in the middle of the loop. In that case, if we have correctly identified the vortex contribution, then

$$< \mathrm{Tr} \exp[i \oint dx^\mu \delta A_\mu^{(n)}] > \ \approx \ < \mathrm{Tr} \exp[i \oint dx^\mu \delta A_\mu^{(0)}] > \tag{19}$$

for sufficiently large loops, and eq. (15) follows immediately. The validity of eq. (15) then constitutes a test of whether P-vortices, which we are using to select the subscript n of $W_n(C)$, actually locate center vortices in the unprojected configurations.

Figure 1 shows the ratio W_1/W_0, with the single P-vortex associated with W_1 located at (or touching) the center of the loop. Likewise, Fig. 2 shows the ratio W_2/W_0, with the two P-vortices for W_2 located near the center of the loop. Both figures were obtained from a simulation on a 14^4 lattice at $\beta = 2.3$ (400 configurations separated by 100 sweeps), and both appear to be quite consistent with the limiting behavior (15).[2]

For very large loops, the fraction of configurations in which no vortex pierces the loop (the subensemble used to compute W_0) becomes very small. So as a further check, using *all* the configurations, we define $W_{evn}(C)$ to be the Wilson loop evaluated in sub-ensemble in which only even (including zero) numbers of P-vortices pierce the minimal area, while $W_{odd}(C)$ is the corresponding quantity for odd numbers of P-vortices. For a very large loop, the fraction of configurations used to evaluate $W_{evn}(C)$, denoted $P_{evn}(C)$, and the fraction $P_{odd}(C)$ used to evaluate $W_{odd}(C)$, should each approach 50% of the total configurations. This is in fact the case, as seen in Fig. 3. If P-vortices in the projected lattice are associated with center vortices in the unprojected lattice, then we would expect, by the same argument leading to eq. (15), that

[2]Qualitatively similar results were found in the indirect maximal center gauge [1].

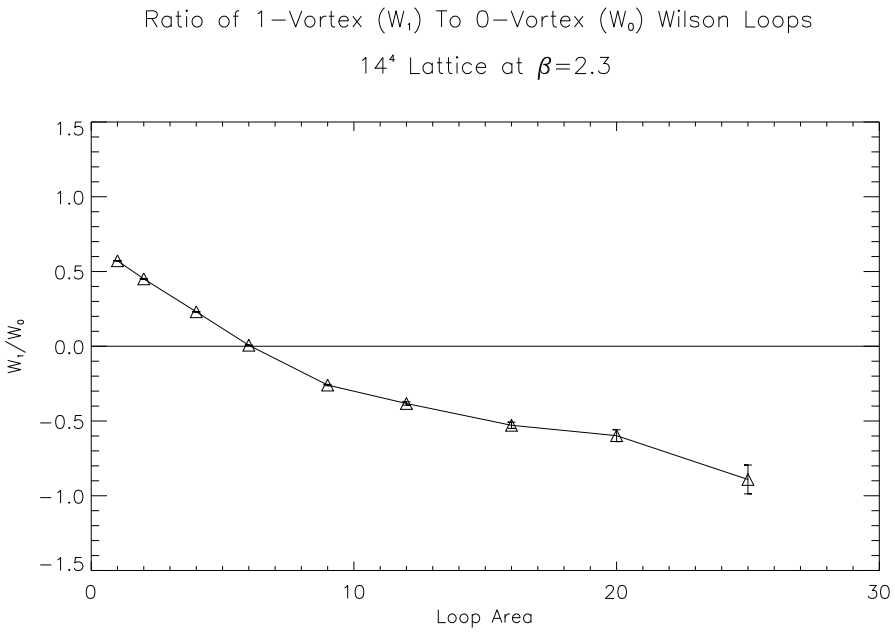

Figure 1: Ratio of the 1-Vortex to the 0-Vortex Wilson loops, $W_1(C)/W_0(C)$, vs. loop area at $\beta = 2.3$.

$$W_{odd}(C) \to -W_{evn}(C) \tag{20}$$

in the limit of large loop area. That also appears to be the case, as seen in Fig. 4.

The conclusion is that P-vortices in center-projected lattice configurations obtained in direct maximal center gauge serve to locate thick center vortices in the full, unprojected, lattice gauge field configuration. It is well to bear in mind, however, that we have no real understanding of *why* this technique finds center vortices; our confidence is based entirely on the numerical results shown in this and the following sections.

2.3 No vortices means no area law

The fact that center vortices can be identified in the gauge-field vacuum does not necessarily imply that vortices are important for the confinement mechanism. There is, however, a simple test of their relevance. Let us define $\chi_n(I, J)$ as the Creutz ratio extracted from the vortex-limited loops $W_n(C)$. If the presence or absence of center vortices crossing the minimal spanning surface of a loop is unrelated to the area-law falloff, then we would naturally expect, at least for large loops, that

$$\chi_0(I, J) \approx \chi(I, J) \tag{21}$$

where $\chi(I, J)$ is the usual Creutz ratio with no restriction on numbers of vortices. In fact, the above equation is entirely wrong, as seen in Fig. 5. When Wilson loops are evaluated

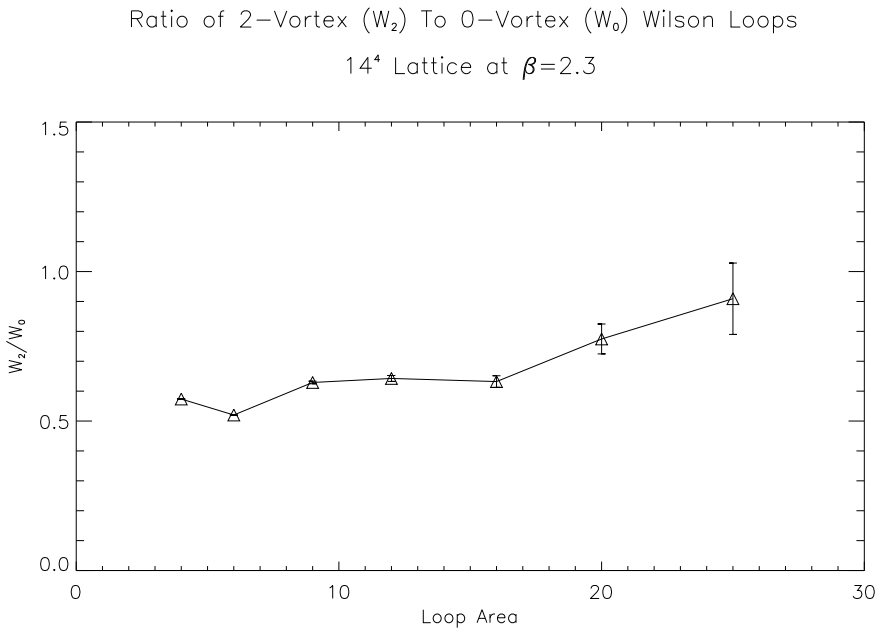

Figure 2: Ratio of the 2-Vortex to the 0-Vortex Wilson loops, $W_2(C)/W_0(C)$, vs. loop area at $\beta = 2.3$.

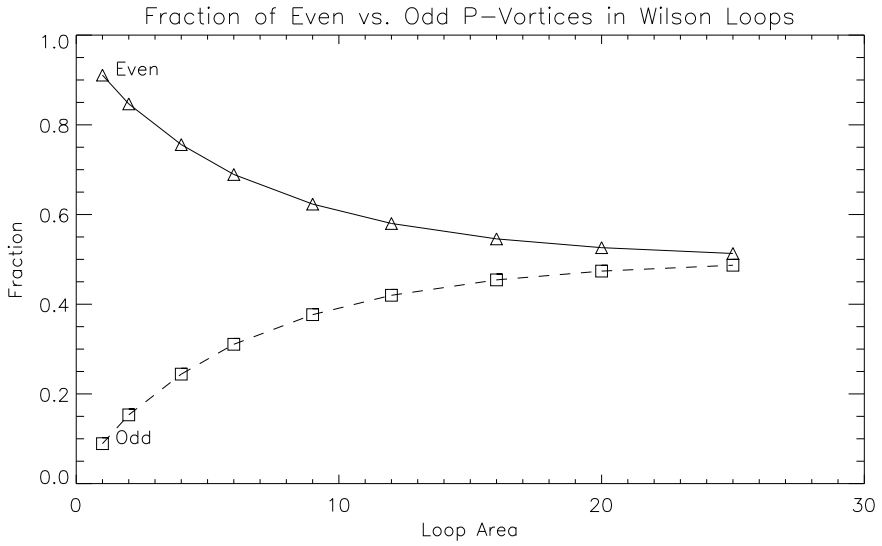

Figure 3: Fraction of link configurations containing even (or zero)/odd numbers of P-vortices, at $\beta = 2.3$, piercing loops of various areas.

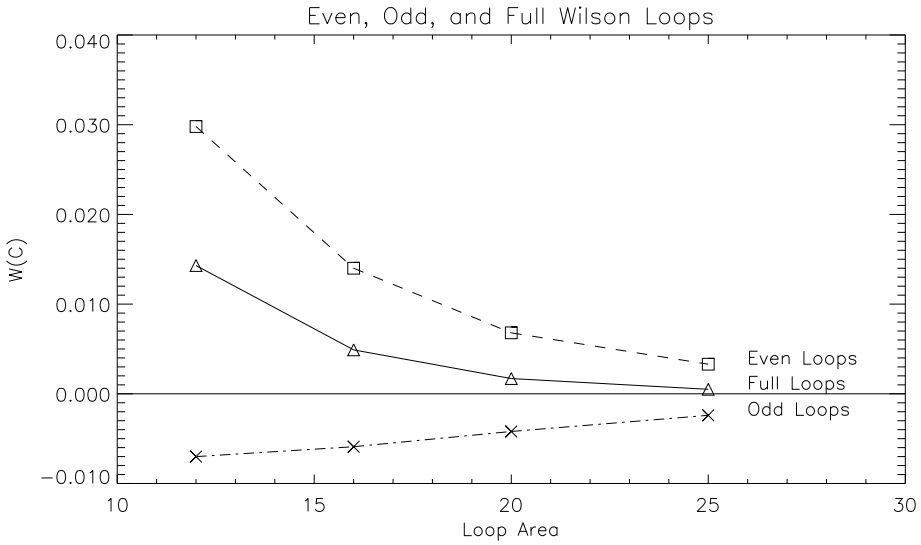

Figure 4: Wilson loops $W_{evn}(C)$, $W_{odd}(C)$, and $W(C)$ at larger loop areas, extracted from configurations with even (or zero) numbers of P-vortices, odd numbers of P-vortices, any any number of P-vortices, respectively, piercing the minimal loop area, again at $\beta = 2.3$.

in subensembles in which no vortices cross the minimal area of the loop, the string tension vanishes.

As a further test, we may consider loops pierced by even (or zero) numbers of vortices. According to the center vortex theory, the asymptotic string tension is entirely due to fluctuations in the number of center vortices piercing the surface of the loop. The asymptotic effect of creating a vortex piercing (once or an odd number of times) the loop surface is to multiply the loop by a center element, i.e. in $SU(2)$

$$\mathrm{Tr}[UU...U] \to (-1) \times \mathrm{Tr}[UU...U] \tag{22}$$

and therefore the area-law falloff is due, asymptotically, to a delicate cancellation between configurations with even (or zero) numbers of vortices piercing the loop (which gives a positive average contribution), and configurations with odd numbers of vortices piercing the loop (which gives a negative average contribution). In fact, we have already seen some evidence of this cancellation in Fig. 4, where the value of the full loop $W(C)$ is much smaller than the magnitudes of either the even or the odd components $W_{evn}(C)$, $W_{odd}(C)$. More quantitatively, if we evaluate Creutz ratios $\chi_{evn}(I, J)$ evaluated from the even-vortex (W_{evn}) contribution alone, the vortex theory predicts that

$$\chi_{evn}(I, J) \to 0 \tag{23}$$

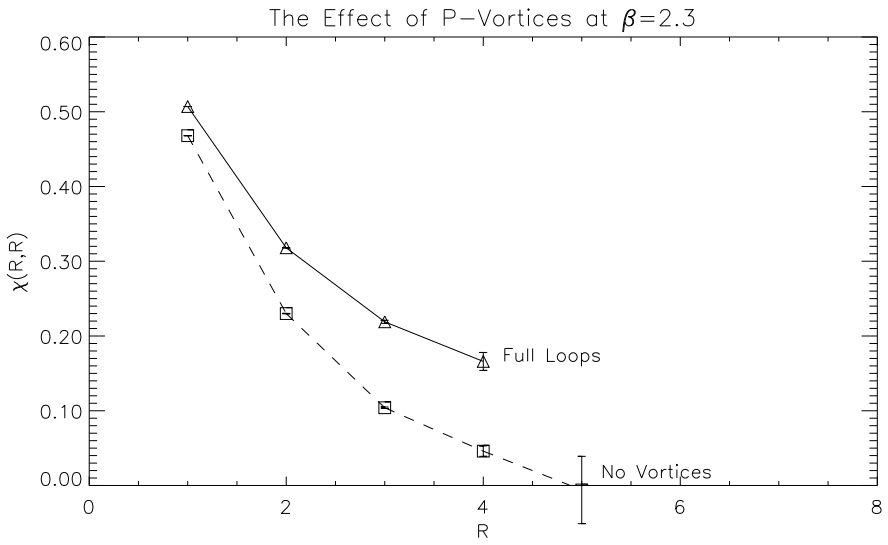

Figure 5: Creutz ratios $\chi_0(R,R)$ extracted from loops with no P-vortices, as compared to the usual Creutz ratios $\chi(R,R)$ at $\beta = 2.3$.

in the limit of large loop area. Once again, from Fig. 6, this appears to be exactly what happens.

2.4 Center vortices generate the full asymptotic string tension

From the previous results, we deduce that the confining properties of lattice gauge-field configurations are strongly correlated with distribution of center vortices. The final check is whether these vortices account for the *entire* asymptotic string tension, as predicted by the center vortex theory. We have already seen that the asymptotic effect of n vortices piercing the middle of a large loop is to contribute a factor $(-1)^n$ to the loop value. In that case, the expectation value of a large Wilson loop can be factored into two components: (i) a factor $W_{vor}(C)$ due to the effect of vortices crossing the minimal area, far from the perimeter of the loop; and (ii) a factor $W_{per}(C)$ due to short-range fluctuations (denoted $\delta A^{(n)}$ in eq. (17)) around the vortex background, near the loop perimeter. Asymptotically, for large-area loops, the vortex theory predicts that

$$\begin{aligned} W(C) &\rightarrow W_{vor}(C) W_{per}(C) \\ W_{vor}(C) &= <(-1)^n> \quad n = \text{no. of vortices piercing C} \end{aligned} \tag{24}$$

Since $W_{per}(C)$ should behave asymptotically like $W_{evn}(C)$ or $|W_{odd}(C)|$, it does not have an area-law falloff, and the entire string tension must be due to $W_{vor}(C)$. But if, as we

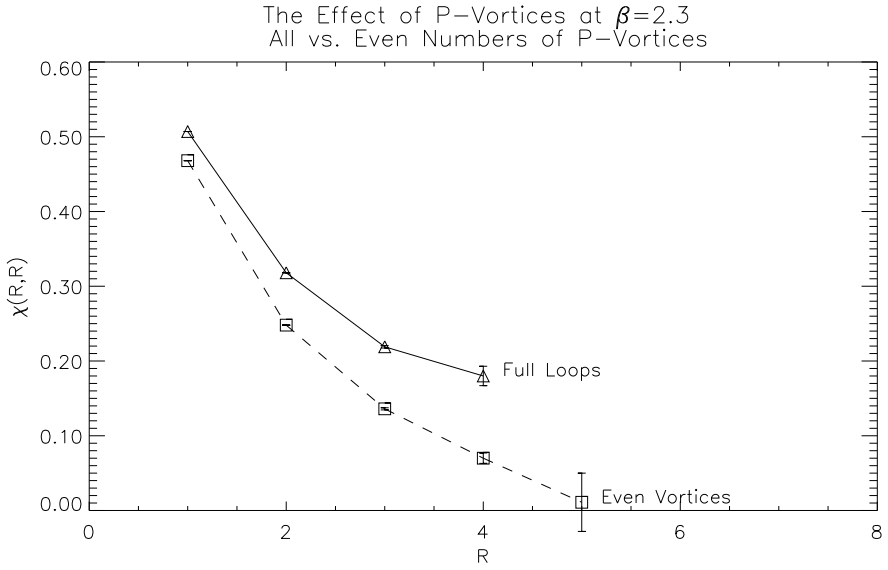

Figure 6: Creutz ratios $\chi_{evn}(R,R)$ extracted from loops $W_{evn}(C)$, taken from configurations with even (or zero) numbers of P-vortices piercing the loop. The standard Creutz ratios at this coupling ($\beta = 2.3$) are also shown.

have seen in the previous section, P-vortices locate center vortices, then

$$W_{vor}(C) =< ZZZ...Z > \quad \text{(center-projected loop value)} \tag{25}$$

where the product of links $ZZ...Z$ on the projected lattice is taken around loop C. Therefore,

- *if* P-vortices locate center vortices, and
- *if* the center vortex theory is correct;
- *then* the string tension of center projected loops should exactly match the asymptotic string tension of the full theory.

Figure 7 is a Creutz ratio plot, extracted from center-projected Wilson loops (i.e. from loops of the $Z_\mu(x)$ link variables) in direct maximal center gauge. The straight solid line is the usual two-loop expression (σ = string tension, a = lattice spacing)

$$\sigma a^2 = \frac{\sigma}{\Lambda^2}\left(\frac{6\pi^2}{11}\beta\right)^{102/121} \exp\left[-\frac{6\pi^2}{11}\beta\right] \tag{26}$$

with $\sigma/\sqrt{\Lambda} = 58$. There are two aspects of this plot which are worth noting in particular. First, unlike a standard plot in the unprojected theory, the Creutz ratios almost fall on

top of one another, starting at $R = 2$. This is not so surprising, from the point of view of the vortex theory. The short range gluonic fluctuations which give rise to the Coulombic potential have been eliminated (these would contribute to $W_{per}(C)$); only the fluctuations in vortex number, which give rise to a linear potential, remain. Second, even $\chi(1,1)$, which is just the logarithm of the center-projected plaquette, appears to be scaling. This fact, as we will see, is related to the scaling of the vortex density.

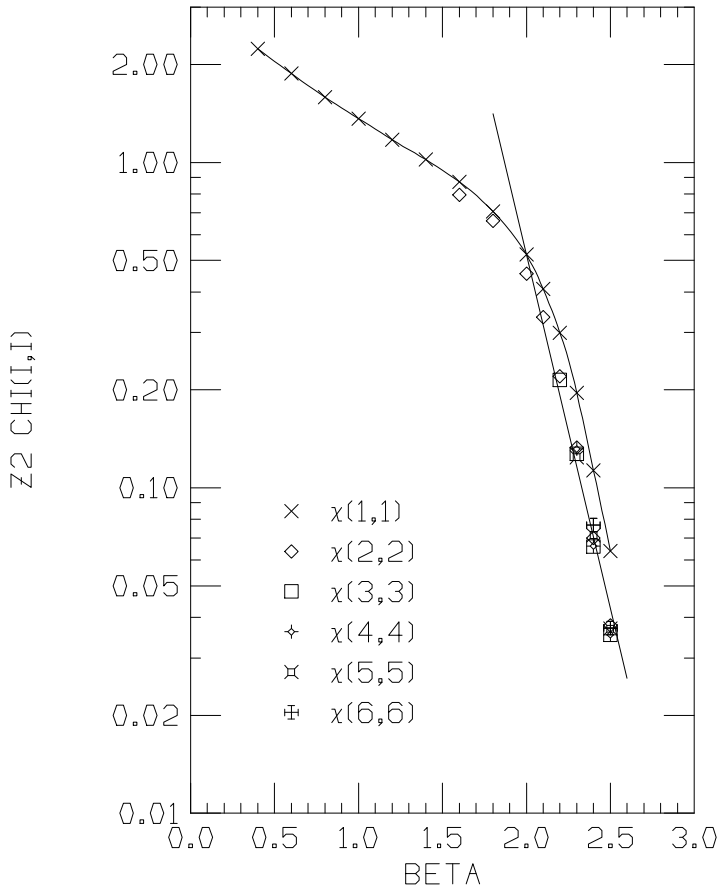

Figure 7: Creutz ratios from center-projected lattice configurations, in the direct maximal center gauge.

Scaling of the center-projected string tension is not sufficient for our purposes; what is necessary is that the actual *value* of the string tension, at every β, agrees with the value for the asymptotic string tension of the unprojected configurations. This is also what we find. Figure 8 shows our data (triangles) in the scaling region, for Creutz ratios $\chi(R,R)$ of center-projected Wilson loops, as compared to the value for the full theory of the asymptotic string tension.[3] The values for the full theory (solid lines), with associated error bars (dashed lines), are taken from Bali et al. [14]. This agreement of the center-

[3]This data was taken, for $\beta = 2.3$ and $\beta = 2.4$, on 16^4 lattices with 30 configurations separated by 100 sweeps. A 22^4 lattice and 20 configurations separated by 100 sweeps was used for $\beta = 2.5$.

projected and full asymptotic string tension persists into the strong coupling regime (see Fig. 17 below).

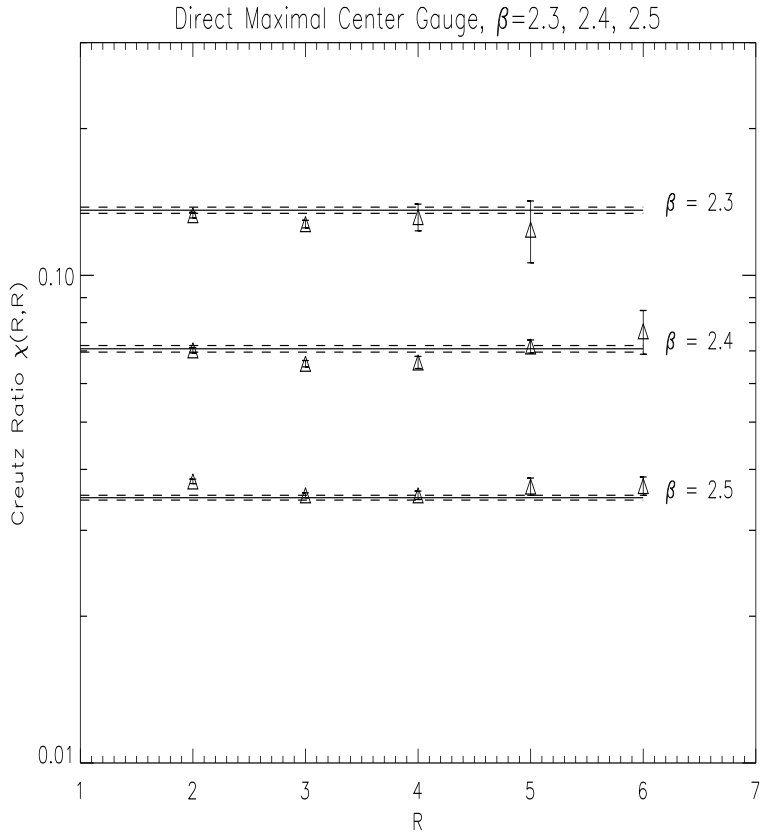

Figure 8: Center-projection Creutz ratios $\chi(R,R)$ vs. R at $\beta = 2.3,\ 2.4,\ 2.5$. Triangles are our data points. The solid line shows the value (at each β) of the asymptotic string tension of the unprojected configurations, and the dashed lines the associated error bars, quoted in ref. [14].

2.5 Scaling of the center vortex density

Finally, we consider the density of vortices. In the vortex theory of confinement, vortices must be "condensed" in the sense that the average extension of a vortex is on the order of the lattice size itself. Its easy to see why. Suppose the opposite were true, i.e. that there were some upper limit to vortex extension, and that almost all vortices, in a very large lattice, would fit inside a hypercube of side length L. Now consider $R \times T$ Wilson loops with $R, T >> L$. Then only vortices within a distance L of the loop perimeter could be linked to the loop, and this would lead asymptotically to a perimeter-law, rather than area-law, falloff.

If vortices are physical objects, their density should scale with β in some appropriate way. P-vortices are located somewhere near the middle of "thick" center vortices in the unprojected lattice, and these P-vortices have the topology of surfaces in D=4 dimensions. If center vortices scale correctly, P-vortices should also scale. The proper asymptotic scaling of P-vortex densities in the *indirect* maximal center gauge was reported recently by Langfeld et al. [15]. We can also observe this scaling in the direct center gauge in a rather simple way: We first define p to be the fraction, and N_{vor} to be the total number, of center projected plaquettes with value -1. N_{vor} is also the total area of all P-vortices on the dual lattice, and we denote by N_T the total number of all plaquettes on the lattice. Then

$$\begin{aligned} p &= \frac{N_{vor}}{N_T} = \frac{N_{vor}a^2}{N_T a^4} a^2 \\ &= \frac{\text{Total Vortex Area}}{6 \times \text{Total Volume}} a^2 \\ &= \frac{1}{6}\rho a^2 \\ &= \frac{1}{6}\frac{\rho}{\Lambda^2}\left(\frac{6\pi^2}{11}\beta\right)^{102/121} \exp\left[-\frac{6\pi^2}{11}\beta\right] \end{aligned} \tag{27}$$

where a is the lattice spacing. The upshot is that p, which is the fraction of plaquettes pierced by P-vortices (equals the probability that any given plaquette is pierced by a P-vortex) should scale like the string tension.

Return now to the Creutz ratio plot in Fig. 7, and in particular the data for the center-projected $\chi(1,1)$, where

$$\chi(1,1) = -\log W_{cp}(1,1) \tag{28}$$

where the "cp" subscript indicates that this is the center-projected Wilson loop. It is easy to see that

$$W_{cp}(1,1) = (1-p) + p \times (-1) = 1 - 2p \tag{29}$$

so for small p (large β) we have

$$\chi(1,1) \approx 2p \tag{30}$$

From the behavior of $\chi(1,1)$, which seems to (at least roughly) parallel the straight line shown, we see that p does appear to scale correctly. However, since (30) is approximate, it is better to plot the precise value of the P-vortex density

$$p = \frac{1}{2}(1 - W_{cp}(1,1)) \tag{31}$$

versus coupling β, as shown in Fig. 9. The straight line is the asymptotic freedom expression (last line of eq. (27)), with the choice $\sqrt{\rho/(6\Lambda^2)} = 50$. The scaling of P-vortex densities, at the larger β values, is rather compelling. There seems little doubt that P-vortices are locating physical, surface-like objects in the full Yang-Mills vacuum; objects which we have identified, in section 2.2 above, as center vortices.

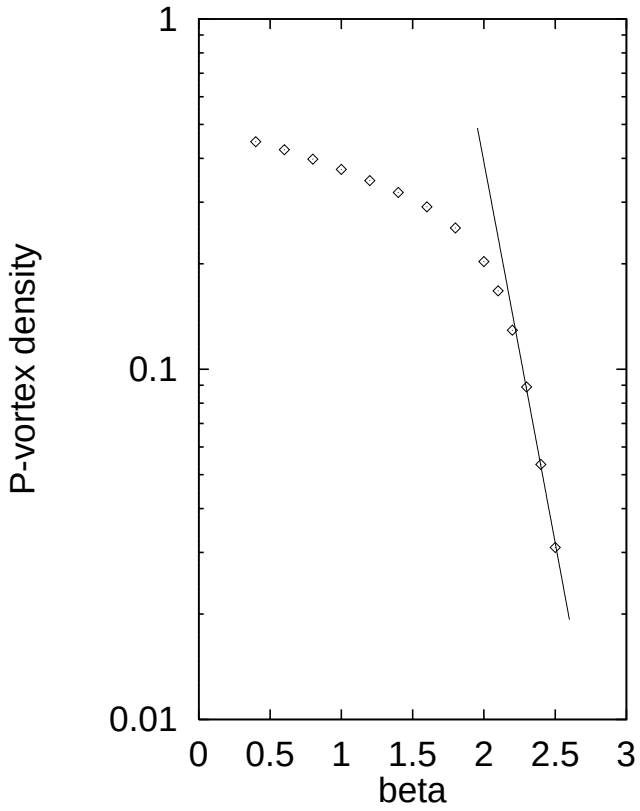

Figure 9: Evidence for asymptotic scaling of the P-vortex density, defined as the fraction p of plaquettes pierced by P-vortices (one-sixth the average area occupied by P-vortices per unit lattice volume). The solid line is the asymptotic freedom prediction of eq. (27), with constant $\sqrt{\rho/(6\Lambda^2)} = 50$.

3 Cooled Vortices

It has been argued persuasively by Teper [16] that the lattice cooling procedure can never, in a finite number of cooling steps, remove the asymptotic string tension extracted from sufficiently large Wilson loops. However, as the number of cooling steps increases, the area-law falloff sets in at increasingly large loop sizes; this means that for a lattice of any fixed volume, confinement is eventually lost. We would like to understand, in the vortex picture, how it is that the area law is lost for smaller loops while being preserved for larger loops, after a finite number of cooling steps.

To answer this question, we need to know what happens to vortices as the lattice is cooled. As before, we use P-vortices found on the uncooled lattice to locate the center vortices, and to count the number of times n that vortices pierce a given lattice surface. The lattice is then cooled, using the constrained cooling procedure of Campostrini et al. [17], and we can study what has happened to the configurations identified on the uncooled lattice. The first quantity of interest is W_1/W_0, where the Wilson loops are evaluated on

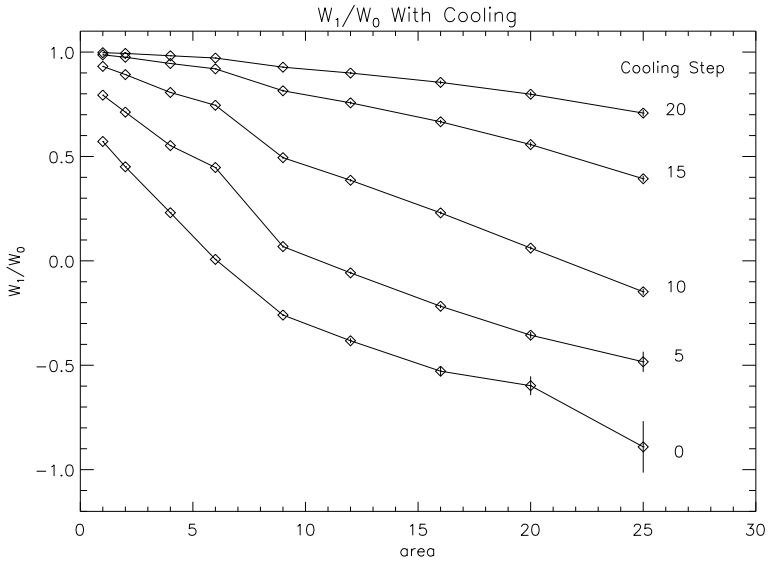

Figure 10: Variation of the ratio W_1/W_0 with the number of cooling steps.

subensembles of the cooled, unprojected lattice, and the P-vortices are identified on the uncooled lattice. The result, from 0-20 cooling steps at $\beta = 2.3$, is shown in Fig. 10 (all data in this section was obtained on a 16^4 lattice). A rough guide to the thickness of a vortex is the loop size for which $W_1/W_0 \approx 0$. According to Fig. 10, this happens for 2×3 loops at cooling step 0, 3×4 loops at cooling step 5, and 4×5 loops at cooling step 10. The simplest interpretation is that the vortices become thicker as the cooling proceeds, with W_1/W_0 reaching its asymptotic value at ever larger distance scales.

The thickening of vortices with cooling explains how the area law is lost for smaller loops, but retained asymptotically for sufficiently large loops. The asymptotic string tension is only obtained for loops whose dimensions are significantly larger than the vortex thickness; there is no area law falloff for loops whose size is very much *smaller* than the vortex thickness.[4] Thus, as cooling begins, loops whose size is comparable to the vortex thickness lose their area-law falloff while the string tension of larger loops is unchanged. As cooling proceeds, vortex thickness increases, and the area law is lost for still bigger loops. However, after any number of cooling steps, there will always be loops (on a sufficiently large lattice) whose extension is large compared to the cooled vortex thickness, and whose asymptotic string tension is untouched.

This picture is supported by the data for $\chi_0(R,R)$ vs. $\chi(R,R)$ after 5 cooling steps (Fig. 11), and after 10 cooling steps (Fig. 12), again at $\beta = 2.3$. These figures should be compared with Fig. 5 above, which shows the same quantities on an uncooled lattice. We notice, particularly after 10 cooling steps, that the Creutz ratios for small loops have been drastically reduced. However, as R increases, the standard Creutz ratio $\chi(R,R)$ rises and seems to level out near the usual value of the asymptotic string tension at $\beta = 2.3$. On the

[4]This point is discussed in much more detail in ref. [9].

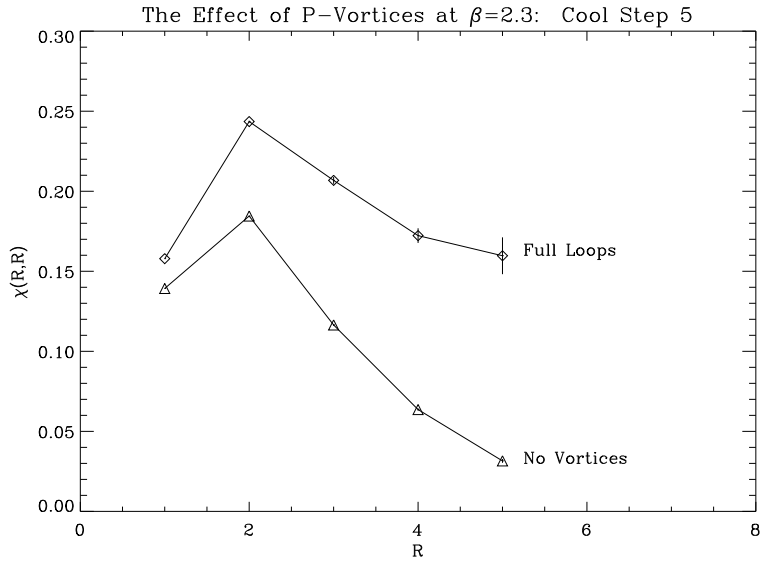

Figure 11: Zero vortex Creutz ratio $\chi_0(R,R)$ and the full Creutz ratio $\chi(R,R)$ vs. R, after 5 cooling steps.

other hand, the zero-vortex Creutz ratio $\chi_0(R,R)$ is again tending to zero for large loops. At 0 cooling steps (Fig. 5), $\chi_0(R,R) \approx 0$ at $R = 5$. At 5 and 10 cooling steps, $\chi_0(5,5) > 0$, although the trend towards zero at increasing loop size is clear. A rough guess is that $\chi_0(R,R) \approx 0$ for R such that $W_1/W_0 \approx -1$.

The message of figures 10-12 is that the vortices are still present on cooled lattices, and are still essential to confinement. However, the asymptotic values $W_1/W_0 \to -1$ and $\chi_0 \to 0$ are obtained only at increasingly large loop area, as the number of cooling steps increases. This behavior, as well as the loss of area law falloff for smaller loops with cooling, seems to be nicely explained as being due to the "thickening" of the vortex core (which is the region of the center vortex which cannot be represented by a gauge transformation with discontinuity (16)).

As just explained, our strategy is to locate the configurations of interest on the uncooled lattice, and then study what happens to these configurations as the lattice is cooled. But it is also interesting to ask whether our procedure for finding the center vortices, i.e. maximal center gauge combined with center projection, also works on the cooled lattices. The answer is "no." In Fig. 13 we show how the P-vortex density p of eq. (27) falls drastically with cooling, if the P-vortices are identified by gauge-fixing and center-projecting the cooled lattice. A corresponding falloff is found in the Creutz ratios $\chi_{cp}(R,R)$ of center-projected loops, with increasing cooling step, as seen, e.g., in Fig. 14 for $R = 5$. There is no trace of the typical "plateau" in string tension over some finite number of cooling steps, found in plotting the usual Creutz ratios. We have also computed $\chi_{cp}(R,R)$ on lattices that have been "smoothed" according to the procedure in ref. [18], and find that the center-projected Creutz ratios are reduced by about a factor of three on the smoothed lattices, as compared

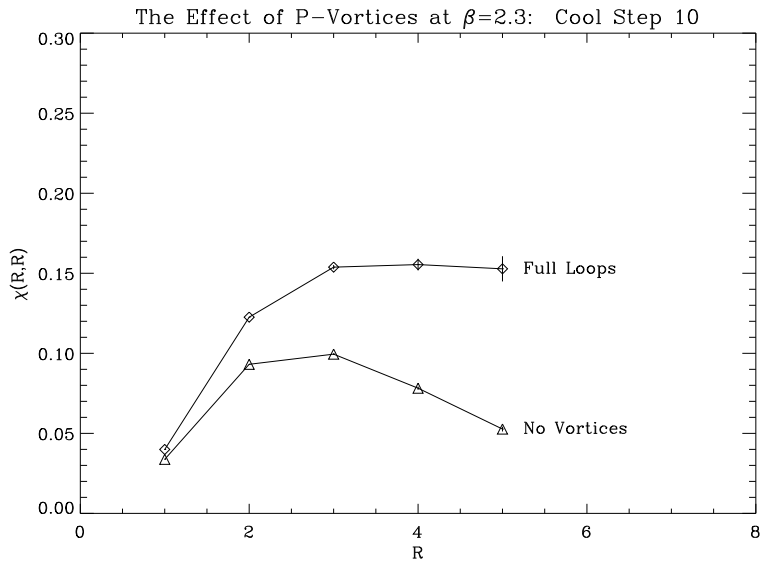

Figure 12: Same as the previous figure, after 10 cooling steps.

to the original lattices.[5] Very similar phenomena have been reported in maximal abelian gauge, in refs. [19, 20].

We stress, however, that the center vortices themselves, on a large lattice, are not removed by cooling. That fact seems evident in Fig. 10-12. What *is* lost on the cooled lattice is the efficacy of center-projection in finding all of the vortices. This suggests that our procedure for locating center vortices is sensitive not only to long-range fluctuations, but also to short-range features of some kind that are associated with these vortices. It would be interesting to know what these short-range features are.[6] This question is under investigation, and we hope to return to it in a future publication.

4 Gribov Copies

The over-relaxation method of gauge-fixing, described in section 2, is not guaranteed to find the absolute maximum of the quantity R in eq. (4); in general it will only find a local maximum. This is the well known "Gribov problem," which also afflicts the Coulomb, Landau, and maximal abelian gauges. It was in order to alleviate the problem that we have made three random gauge copies of each configuration used for data taking, and gauge-fixed each to obtain three "Gribov copies." We then used the Gribov copy with the largest value of R.

Since Gribov copies of a given lattice configuration are not identical, it is interesting to study by how much, on average, they differ. In particular, to what extent are the

[5] We thank T. Kovács for kindly supplying us with 100 smoothed lattice configurations.

[6] One clue is that the unprojected plaquette energy at the location of P-vortices, in the uncooled lattice, is significantly higher than the average plaquette energy.

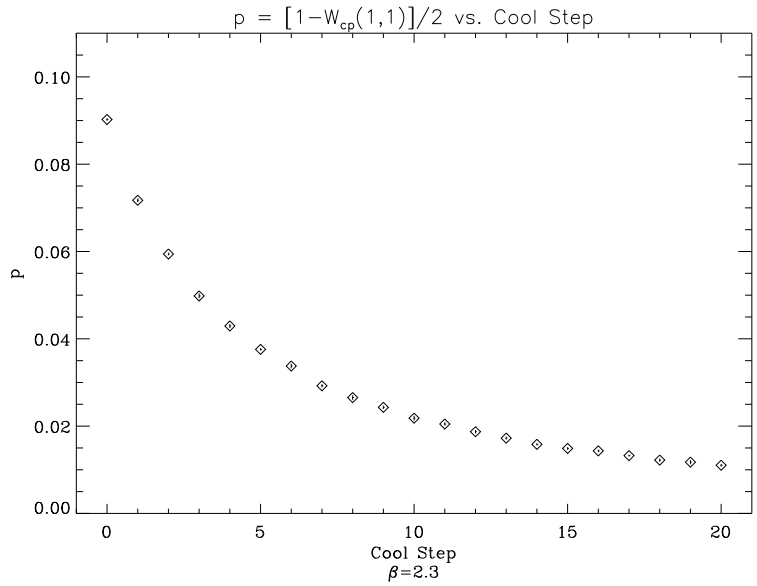

Figure 13: The drop in P-vortex density p, identified by center-projection in maximal center gauge, on cooled lattices.

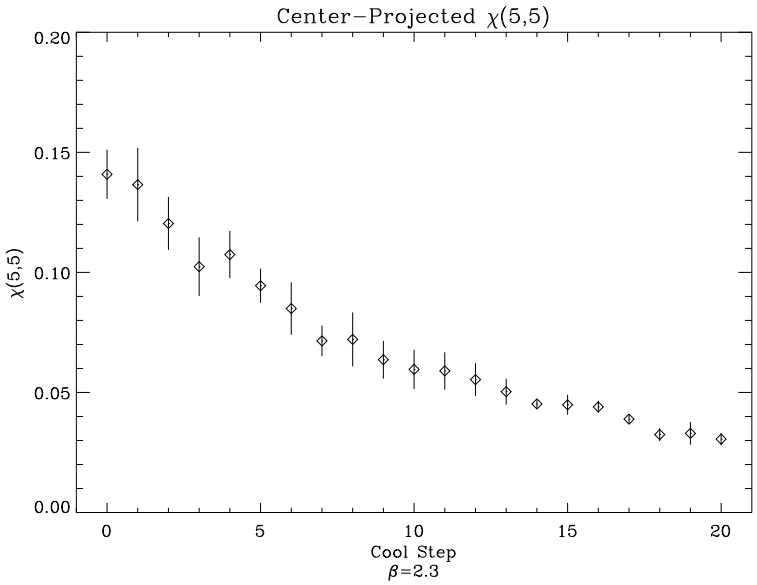

Figure 14: The drop in the center-projected Creutz ratio $\chi_{cp}(5,5)$, corresponding to the drop in p, with cooling step.

positions of P-vortices correlated from copy to copy? If there is no correlation, then we can hardly rely on P-vortices to locate physical objects (i.e. the thick center vortices). On the other hand, some variation in the position of P-vortices, from copy to copy, should be permissible. Center vortices are rather thick, extended objects, and the precise "middle" surface of such configurations, which P-vortices are supposed to locate, may be somewhat ill-defined.

To investigate quantitatively the correlation of vortices in different Gribov copies, we do the following: A Monte Carlo simulation is run at a given β, taking data every 100 sweeps, and making 4 copies of each configuration chosen for data taking. The two "best" Gribov copies (in the sense of having the largest R values) are center-projected, and we denote the projected configurations by $Z'_\mu(x)$ and $Z''_\mu(x)$, with corresponding center-projected Wilson loops

$$\begin{aligned} \mathcal{W}'(C) &= Z'Z'...Z' \\ \mathcal{W}''(C) &= Z''Z''...Z'' \end{aligned} \tag{32}$$

Then we compute the expectation value of the loop product

$$< \mathcal{W}'(C)\mathcal{W}''(C) > \tag{33}$$

If the correlation of P-vortices in the two Gribov copies were perfect, then

$$\mathcal{W}'(C) = \mathcal{W}''(C) = \pm 1 \tag{34}$$

and therefore

$$< \mathcal{W}'(C)\mathcal{W}''(C) >= 1 \qquad \text{perfect correlation} \tag{35}$$

At the other extreme, if there were no correlation at all between the P-vortex positions in the two Gribov copies, then

$$\begin{aligned} < \mathcal{W}'(C)\mathcal{W}''(C) > &= < \mathcal{W}'(C) >< \mathcal{W}''(C) > \\ &= \exp[-2\sigma \text{Area}(C)] \qquad \text{no correlation} \end{aligned} \tag{36}$$

where σ is the string tension of the center-projected loops (same as the asymptotic tension of the unprojected loops).

Small variations in P-vortex position among different Gribov copies are most likely to lead to a perimeter law falloff of the loop product (33), at least in the limit of large loop area. Consider, for example, the following simple model: Take an $I \times J$ Wilson planar loop and assign to each of the plaquettes in its plane, both inside and outside the loop, a value $+1$ with probability $(1-f)$, and -1 with probability f. Each such configuration is supposed to represent a particular "Gribov copy" of center-projected plaquettes in the plane, and the value of the Wilson loop is $\mathcal{W}'_{cp}(I,J) = (-1)^{n'}$, where n' is the number of negative plaquettes in the minimal area. It is not hard to see, since the plaquettes are assumed to be uncorrelated, that, averaging over many configurations gives

$$\begin{aligned} W'_{cp}(I,J) &= < \mathcal{W}'(I,J) > \\ &= (1-2f)^{IJ} = \exp[-\sigma IJ] \end{aligned} \tag{37}$$

where $\sigma = -\log(1-2f)$ (the assumption that nearby plaquettes are completely uncorrelated is the main unrealistic feature of this model). From a given configuration of ± 1 plaquettes, we construct a second "Gribov copy" by allowing negative plaquettes to change their position by, at most, one lattice spacing. Then only changes in position of negative plaquettes bordering the loop perimeter can cause the loop product to differ from $+1$. Assign to a negative plaquette on the perimeter a probability q to cross *into* the loop, if it were outside, or to cross outside the loop, if it were inside.[7] The new value of the loop is $(-1)^{n''}$, where n'' is the number of negative plaquettes inside the loop in the second "Gribov copy." One then finds that in this model, defining $N \equiv 4(I+J)$,

$$\begin{aligned} < \mathcal{W}'(I,J)\mathcal{W}''(I,J) > &= \sum_{n=0}^{N} (1-2q)^n f^n (1-f)^{N-n} \frac{N!}{n!(N-n)!} \\ &= (1-2qf)^{4(I+J)} \end{aligned} \tag{38}$$

which is a perimeter-law falloff.

The above argument should also go through if the P-vortex positions vary by more than one lattice spacing among Gribov copies, so long as the variation is small compared to the size of the loop. If the variation in P-vortex position is comparable to the thickness of the center vortex, then our best chance to see perimeter-law falloff in the loop product (33), for comparatively small-size loops, will be at smaller values of coupling β, where the vortex is relatively thin in lattice units. We have therefore chosen to do our simulation at a value of $\beta = 2.1$ which is just past the strong-to-weak coupling crossover.

Figures 15 and 16 show our Monte Carlo results at $\beta = 2.1$ on a 14^4 lattice, with data from 400 configurations separated by 100 sweeps between configurations. Triangles show the data for loop products $< \mathcal{W}'(C)\mathcal{W}''(C) >$, plotted vs. loop area, while the crosses are the values for no correlation, i.e. $< \mathcal{W}'(C) >< \mathcal{W}''(C) >$. The loop products are clearly far above the uncorrelated value and, from Fig. 15, do not seem consistent with an area-law falloff. In Fig. 16 the loop product is plotted vs. loop perimeter. The straight line is drawn, somewhat arbitrarily, through data points at perimeter $= 10,\ 18$. It appears that the falloff in the loop product with perimeter is quite compatible with perimeter-law falloff, as predicted in our simple model.

These results indicate that the variation in P-vortex position among different Gribov copies is relatively small - perhaps on the order of the vortex thickness, although we have not quantified this - and leads asymptotically only to a perimeter-law falloff for the loop product $< \mathcal{W}'(C)\mathcal{W}''(C) >$, indicating a strong correlation among Gribov copies.

5 First Results in SU(3)

All results presented in the previous sections support the idea that thick Z_2 vortices are *the* configurations dominating the $SU(2)$ Yang–Mills vacuum. However, the vortex mechanism

[7] Plaquettes touching the corners of the loop should be treated a little differently from the other plaquettes along the perimeter, but this is an inessential complication of the model, which we will ignore.

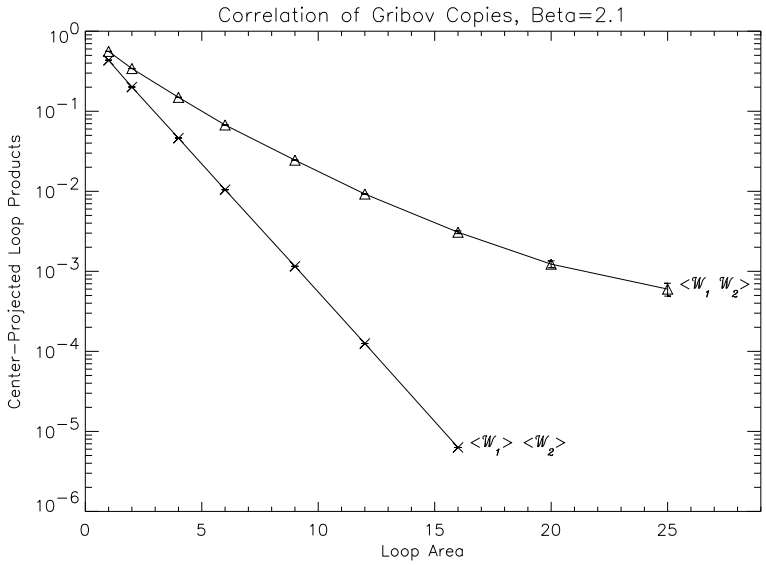

Figure 15: Expectation value of products of center-projected Wilson loops (triangles), evaluated in different Gribov copies, plotted vs. Loop Area. Crosses indicate the value for no correlation.

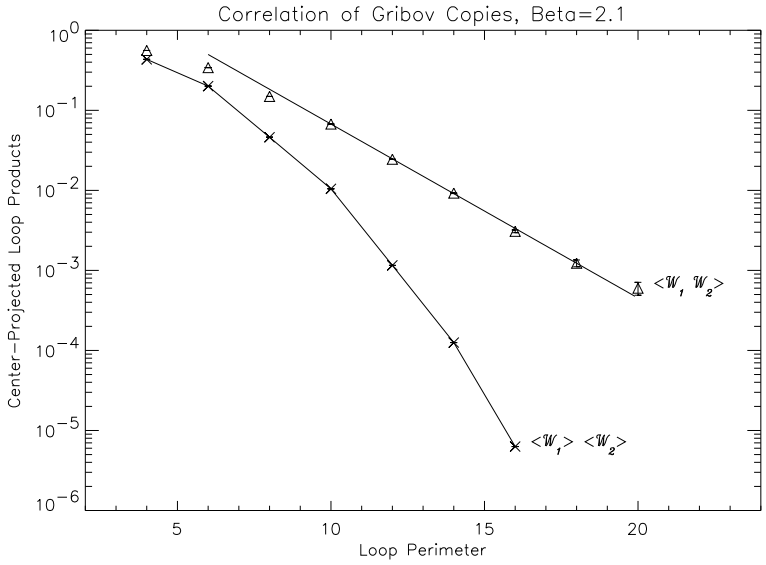

Figure 16: Expectation value of products of center-projected Wilson loops, evaluated in different Gribov copies, plotted vs. Loop Perimeter.

should not be specific to the $SU(2)$ gauge group. In nature quarks appear in three colors, so a very urgent question is whether the observed phenomena survive the transition from $SU(2)$ to $SU(3)$.

The maximal center gauge in $SU(3)$ gauge theory is defined as the gauge which brings link variables U as close as possible to elements of its center $Z_3 = \{e^{-2i\pi/3}I,\ I,\ e^{2i\pi/3}I\}$. This can be achieved e.g. by maximizing the quantity

$$R = \sum_{x,\mu} \mathrm{Re}\left([\mathrm{Tr}\ U_\mu(x)]^3 \right), \tag{39}$$

or

$$R' = \sum_{x,\mu} |\ \mathrm{Tr}\ U_\mu(x)\ |^2\ . \tag{40}$$

We will concentrate here on the first choice. Center projection then amounts to replacing full link variable $U_\mu(x)$ by $Z_\mu(x)$, the closest center element. The residual unfixed local gauge symmetry is that of Z_3.

Fixing to the maximal center gauge in $SU(3)$ gauge theory turns out to be much more difficult and computationally intensive than in the case of $SU(2)$. The reason is that we have not succeeded in reducing the maximization to an underlying linear algebra problem as in $SU(2)$ (see Section 2.1). We thus resorted to the method of simulated annealing [21,22], which was used for maximal abelian gauge fixing by Bali et al. [23]. However, this method of maximal center gauge fixing converges to the maximum of R, Eq. (39), very slowly, which has forced us thus far to restrict simulations to small lattice sizes and to strong coupling. Tests of a more efficient maximization procedure are in progress.

Before discussing the strong coupling results for $SU(3)$, let us first show analogous data from $SU(2)$ gauge theory. In Figure 17 we plot values of center-projected Wilson loops $W(I,J)$ in maximal center gauge for $\beta \leq 2.5$. Broken lines connecting data points are just meant to guide the eye. Solid lines represent result of the lowest-order strong-coupling expansion (for unprojected loops)

$$W(I,J) = \left(\frac{\beta}{4}\right)^{IJ}\ . \tag{41}$$

Monte Carlo data for projected loops agree with the lowest-order strong coupling expansion up to about $\beta = 1.5$.

Our first results from $SU(3)$ lattice gauge theory simulations come from an 8^4 lattice, for β values 1.0, 2.0, 3.0, 4.0, 5.0, 5.4 and 5.6. Figure 18 shows center-projected Wilson loops together with the standard strong-coupling expansion to leading and next-to-leading order:

$$W(I,J) = \left(\frac{\beta}{18}\right)^{IJ} \left(1 + \frac{IJ}{12}\beta + O(\beta^2)\right). \tag{42}$$

The data agree with lowest-order strong-coupling expansion up to $\beta \simeq 2$; when next-to-leading term is taken into account, the agreement extends up to $\beta = 4$.

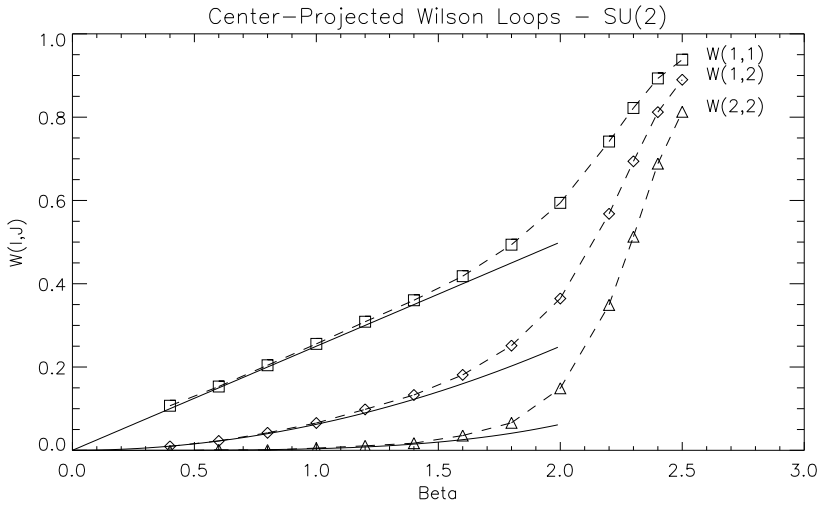

Figure 17: Center-projected Wilson loops vs. the strong-coupling expansion (solid lines) in $SU(2)$ lattice gauge theory

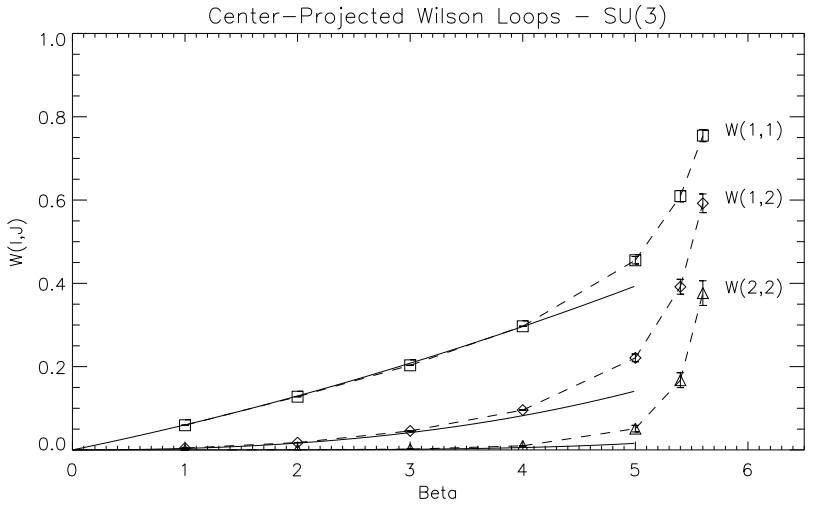

Figure 18: Center-projected Wilson loops vs. the strong-coupling expansion (solid lines) in $SU(3)$ lattice gauge theory

Qualitatively, the situation at strong coupling looks much the same in $SU(2)$ and $SU(3)$: in both cases full Wilson loops are well reproduced by those constructed from center elements alone in maximal center gauge. Thus, center dominance is seen also in $SU(3)$ gauge theory at strong coupling.

An immediate task for the near future is to repeat our investigation of center dominance and the role of vortices in $SU(3)$ lattice gauge theory for couplings in the scaling region. An absolutely crucial check of the validity of the vortex mechanism is that the evidence for vortices found in the $SU(2)$ lattice theory is also found for the $SU(3)$ gauge group.

6 Summary

It may be worth summarizing the results reported here:

- **P-Vortices locate center vortices.** Vortex excitations in the center-projected configurations, in direct maximal center gauge, locate center vortices in the full, unprojected lattice. The evidence for this comes from the fact that $W_n(C)/W_0(C) \to (-1)^n$, and $W_{odd}(C) \to -W_{evn}(C)$ in the limit of large loop area.

- **No vortices $\Rightarrow$ no confinement.** When Wilson loops in $SU(2)$ gauge theory are evaluated in subensembles of configurations with no vortices (or only an even number of vortices) piercing the loop, the string tension disappears.

- **Vortices, by themselves, account for the full string tension.** The string tension of the vortex contribution to Wilson loops is found to match, quite accurately, the asymptotic string tension extracted from the full Wilson loops.

- **Vortex density scales.** The variation of P-vortex density with coupling β goes as expected for a physical quantity with dimensions of inverse area. This is additional evidence that P-vortices locate physical, surface-like objects (center vortices) in the Yang-Mills vacuum (see also ref. [15]).

- **Center vortices thicken as the lattice cools.** This enables us to explain how the area law falloff is lost, after a finite number of cooling steps, for smaller loops, while the string tension remains unchanged for sufficiently large loops.

- **P-vortex locations are correlated among Gribov copies.** There appears to be only modest sensitivity in P-vortex location to the choice of Gribov copy.

- **SU(3).** There is preliminary evidence, on small lattices and strong couplings, of center dominance also in $SU(3)$ lattice gauge theory.

It is also worth mentioning some other results reported in refs. [2, 9]:

- **Monopole loops lie on P-vortices [2].** Monopoles, identified in the maximal abelian gauge, lie along center vortices, found in the indirect maximal center gauge, in a monopole-antimonopole chain. The non-abelian field strength of monopole cubes, above the lattice average, is directed almost entirely along the associated center vortices. Monopoles appear to be rather undistinguished regions of vortices, and may simply be artifacts of the abelian projection, as explained in ref. [2].

- **Center vortices are compatible with Casimir scaling [9].** The "Casimir scaling" of the string tension of higher representation Wilson loops, at intermediate distance scales, has long been considered incompatible with the center vortex theory. Very recently, however, it has been argued that Casimir scaling is explained in terms of center vortices, if we take into account the fact that center vortices, unlike P-vortices, have a thickness which may be much greater than one lattice spacing.[8]

These results support the view that center vortices are responsible for quark confinement.

Acknowledgements

This work was supported in part by PPARC under Grant GR/L56329 (L.DD.), Fonds zur Förderung der Wissenschaftlichen Forschung P11387-PHY (M.F.), the U.S. Department of Energy under Grant No. DE-FG03-92ER40711 and Carlsbergfondet (J. Gr.), the "Action Austria-Slovak Republic: Cooperation in Science and Education" (Project No. 18s41) and the Slovak Grant Agency for Science, Grant No. 2/4111/97 (Š. O.).

J.Gr. and J.Gi. are grateful for the generous assistance of the High Energy Theory Group at Lawrence Berkeley National Laboratory, whose computer facilities were used extensively in this project.

References

[1] L. Del Debbio, M. Faber, J. Greensite, and Š. Olejník, Phys. Rev. D55 (1997) 2298, hep-lat/9610005.

[2] L. Del Debbio, M. Faber, J. Greensite, and Š. Olejník, proceedings of the Zakopane meeting *New Developments in Quantum Field Theory*, hep-lat/9708023;
proceedings of the Buckow meeting *31st Int. Symposium on the Theory of Elementary Particles*, in preparation.

[8] Related work on the adjoint potential, in the context of a particular model of center vortices, may be found in ref. [24]; some speculations about hedgehog solutions, in the same framework, are found in ref. [25]. The approach taken in ref. [24] has some similarities to ours in ref. [9], but also differs in a number of important respects. In particular there is no apparent Casimir scaling found in the former approach, and there also seems to be an explicit conflict with the large-N factorization property at $N_{colors} \to \infty$.

[3] L. Del Debbio, M. Faber, J. Greensite, and Š. Olejník, proceedings of LATTICE 97, hep-lat/9709032.

[4] G. 't Hooft, Nucl. Phys. B138 (1978) 1.

[5] G. Mack, in *Recent Developments in Gauge Theories*, edited by G. 't Hooft et al. (Plenum, New York, 1980).

[6] H. B. Nielsen and P. Olesen, Nucl. Phys. B160 (1979) 380;
J. Ambjørn and P. Olesen, Nucl. Phys. B170 (1980) 60; 265.

[7] J. M. Cornwall, Nucl. Phys. B157 (1979) 392.

[8] R. P. Feynman, Nucl. Phys. B188 (1981) 479.

[9] M. Faber, J. Greensite, and Š. Olejník, hep-lat/9710039, to appear in Phys. Rev. D.

[10] T. Kovács and E. Tomboulis, hep-lat/9711009; hep-lat/9709042.

[11] A. Kronfeld, M. Laursen, G. Schierholz, and U.-J. Wiese,
Phys. Lett. B198 (1987) 516 ;
T. Suzuki and I. Yotsuyanagi, Phys. Rev. D42 (1990) 4257.

[12] L. Del Debbio, M. Faber, J. Greensite, and Š. Olejník, Nucl. Phys. Proc. Suppl. 53 (1997) 141, hep-lat/9607053.

[13] J. E. Mandula and M. Ogilvie, Phys. Lett. B248 (1990) 156.

[14] G. Bali, C. Schlichter, and K. Schilling, Phys. Rev. D51 (1995) 5165.

[15] K. Langfeld, H. Reinhardt, and O. Tennert, hep-lat/9710068.

[16] M. Teper, Nucl. Phys. B411 (1994) 855.

[17] M. Campostrini, A. Di Giacomo, M. Maggiore, H. Panagopoulos, and E. Vicari, Phys. Lett. B225 (1989) 403.

[18] T. DeGrand, A. Hasenfratz, and T. Kovács, Nucl. Phys. B505 (1997) 417, hep-lat/9705009.

[19] A. Hart and M. Teper, hep-lat/9709009.

[20] T. G. Kovács and Z. Schram, Phys. Rev. D56 (1997) 6824, hep-lat/9706012.

[21] V. Černý, Comenius Univ. preprint (1982), J. Opt. The. Appl. 45 (1985) 41.

[22] S. Kirkpatrick, C. D. Gelatt, Jr., M. P. Vecchi, Science 220 (1983) 671.

[23] G. S. Bali, V. Bornyakov, M. Müller-Preussker, and F. Pahl, Nucl. Phys. Proc. Suppl. 42 (1995) 852.

[24] J. M. Cornwall, hep-th/9712248;
and in Proceedings of the *Workshop on Non-Perturbative Quantum Chromodynamics*, edited by K. A. Milton and M. A. Samuel (Birkhauser, Boston, 1983).

[25] J. M. Cornwall and G. Tiktopoulos, Phys. Lett. B181 (1986) 353.